Boundary-Layer Meteorology (2021) 178:185–199
https://doi.org/10.1007/s10546-020-00571-4

RESEARCH ARTICLE

Multi-Point Monin–Obukhov Similarity of Turbulence Cospectra in the Convective Atmospheric Boundary Layer

Mengjie Ding[1] · Chenning Tong[1]

Received: 18 April 2020 / Accepted: 3 September 2020 / Published online: 28 September 2020

Abstract
The shear-stress cospectrum and the horizontal and vertical temperature-flux cospectra in the convective boundary layer (CBL) are predicted using the multi-point Monin–Obukhov similarity (MMO theory). MMO theory was recently proposed and then derived from first principles by Tong and Nguyen (Journal of the Atmospheric Sciences, 2015, Vol. 72, 4337 – 4348) and Tong and Ding (Journal of Fluid Mechanics, 2019, Vol. 864, 640 – 669) to address the issue of the incomplete similarity in the Monin–Obukhov similarity theory. According to MMO theory, the CBL has a two-layer structure: the convective layer ($z \gg -L$) and the convective–dynamic layer ($z \ll -L$). The former consists of the convective range ($k \ll -1/L$) and the inertial range ($k \gg 1/z$), while the latter consists of the convective range, the dynamic range ($-1/L \ll k \ll 1/z$), and the inertial range, where z, k, and L are the height from the ground, the horizontal wavenumber, and the Obukhov length, respectively. We use MMO theory to predict the cospectra for the convective range and the dynamic range. They have the same scaling in the convective range for both $z \ll -L$ and $z \gg -L$. The shear-stress cospectrum and the vertical temperature-flux cospectrum have k^0 scaling in both the convective and dynamic ranges. The horizontal temperature-flux cospectrum has $k^{-1/3}$ and k^{-1} scaling in the convective and dynamic ranges respectively. The predicted scaling exponents are in general agreement with high-resolution large-eddy-simulation results. However, the horizontal temperature-flux cospectrum is found to change sign from the dynamic range (negative) to the convective range (positive), which is shown to be caused by the temperature–pressure-gradient interaction.

Keywords Atmospheric flows · Boundary-layer structure · Turbulence

1 Introduction

The Monin–Obukhov similarity theory (MOST; Obukhov 1946; Monin and Obukhov 1954;) is the foundation for understanding the atmospheric surface layer. MOST hypothesizes that nondimensional turbulence statistics in the surface layer depend only on the nondimensional parameter z/L, where $L = -u_*^3/(\kappa(g/\Theta)Q)$, with z, L, u_*, κ, g, Θ, and Q being the

✉ Chenning Tong
ctong@clemson.edu

[1] Department of Mechanical Engineering, Clemson University, Clemson, South Carolina 29634, USA

height from the ground, the Obukhov length, the friction velocity, the von Kármán constant, the acceleration due to gravity, the mean potential temperature, and the surface temperature flux, respectively. Many important surface-layer statistics have been found to conform to MOST, such as the non-dimensional mean shear and potential temperature gradients, the turbulence kinetic energy budget, the vertical velocity variance, and the inertial-range spectra and cospectra (e.g., Businger et al. 1971; Wyngaard and Coté 1971; Wyngaard et al. 1971; Kaimal et al. 1972; Kaimal 1978; Högström 1988, 1990). However, it has also been known since the late 1950s that a number of important surface-layer statistics, such as the horizontal velocity variances and the large-scale horizontal velocity spectra, do not conform to MOST (e.g., Lumley and Panofsky 1964; Zilitinkevich 1971; Betchov and Yaglom 1971; Kaimal et al. 1972; Kaimal 1978; Caughey and Palmer 1979; Kader 1988; Yaglom 1994). The non-MOST behaviour renders the surface-layer similarity in the MOST framework incomplete, raising questions about the existence of general similarity in surface layer.

The multi-point Monin–Obukhov similarity (MMO) theory was proposed to address the issue of incomplete similarity in MOST (Tong and Nguyen 2015). They showed that the incomplete similarity was related to two assumptions used in MOST: (1) the length scale of the energy-containing eddies is z, and (2) L is only a vertical length scale. However, for some important statistics in a convective surface layer (e.g., the horizontal velocity variances), z is not the proper scale for the energy-containing motions. The scales of convective eddies at a height z range from z to z_i, where z_i is the boundary-layer (capping-inversion) height. Consequently, for these statistics the length scale of the energy-containing eddies is not properly represented in MOST. To represent the length scale, the scales of turbulent eddies must be explicitly included in a new similarity theory. Therefore, multi-point statistics, which are functions of the separations between multiple points, need to be used to formulate the theory. Furthermore, Tong and Nguyen (2015) argued that the Obukhov length L is not only a vertical length scale, but also a horizontal length scale, which was suggested by the new understanding of the surface-layer physics gained in their AHATS field campaign (Nguyen 2015; Nguyen and Tong 2015), which showed that fluctuations of wavenumber k at the height $z \sim 1/k$ are coupled to those of k at $z \ll 1/k$ by the large convective eddies through the pressure transport and the pressure–strain-rate correlation. As a result, the buoyancy effects are also important at a height $z \ll -L$ for wavenumbers $k \ll -1/L$. This indicates that L is also a length scale in the horizontal direction, and $-kL$ is another non-dimensional parameter for the complete similarity in addition to z/L.

MMO theory hypothesizes that complete similarity can only be achieved by multi-point statistics, which, when non-dimensionalized using the surface-layer parameters, depend only on the non-dimensional parameters z/L and $-kL$. Tong and Nguyen (2015) used the joint probability density function of velocity differences to formulate MMO theory, hypothesizing that all multi-point velocity difference statistics have similarity properties. MMO theory predicts that the convective surface layer has a two-layer structure (i.e., MMO scaling region in Fig. 1): the convective layer ($z \gg -L$) and the convective–dynamic layer ($z \ll -L$). Two spectral scaling ranges were discovered in the convective–dynamic layer: the convective range ($k \ll -1/L$), in which the eddies are dominated by the buoyancy effects and the dynamic range ($k \gg -1/L$), in which the eddies are dominated by the shear effects. As an application of MMO theory, the velocity and temperature spectra in the convective atmospheric surface layer were predicted. The horizontal and vertical velocity spectra and the temperature spectrum have $k^{-5/3}$, $k^{1/3}$ and $k^{-1/3}$ wavenumber dependencies in the convective range, respectively, and have k^{-1}, k and k^{-1} dependencies in the dynamic range, respectively. A preliminary comparison with large-eddy simulation (LES) results showed good agreement.

Within the MMO framework, similarity of one-point statistics, regardless of whether they follow MOST or not, can be derived from their relationships with multi-point statistics. For example, scaling of the velocity variances can be obtained from the scaling of the velocity spectra. The similarity properties of mean gradients can be obtained through equations containing mean gradient terms, such as the shear-stress budget equation, which contains a mean-shear term (Tong and Ding 2020). The scaling of the budget equations is obtained using the MMO theory. In this regard, MOST can be regarded a special case of MMO theory.

MOST and MMO theory were proposed as hypotheses based on phenomenology. Measurements can provide support to them, but cannot positively prove them. However, we have recently analytically derived the surface-layer similarity from first principles. As a result, the MMO theory is no longer a hypothesis. Tong and Ding (2018) used the method of matched asymptotic expansions to derive the Monin–Obukhov similarity for the vertical velocity and potential temperature variances. The equations of the vertical velocity and potential temperature variances were employed in the analysis. The equations were shown to form a singular perturbation problem in the vertical direction, with two layers dominated by the buoyancy production and shear production, respectively. The Obukhov length L was shown analytically to be a length scale in the vertical direction. The local-free-convective scaling (Wyngaard et al. 1971) was derived by matching the two layers. Tong and Ding (2019) analytically derived the MMO theory from first principles using the method of matched asymptotic expansions. The Navier–Stokes equations and the potential temperature equation in Fourier space were employed in the analysis. They showed that for the large-scale convective motions ($k < -1/L$), the solution is uniformly valid in the z direction, with the scaling unchanged as z decreases from $z > -L$ to $z < -L$. In the convective–dynamic layer ($z < -L$), as k increases from $k < -1/L$ to $k > -1/L$, the scaling changes, resulting in a singular perturbation problem. Therefore, L was shown analytically to be also a length scale in the horizontal direction, and $-kL$ enters as a new non-dimensional parameter. From the singularity in the wavenumber (k) direction, the convective–dynamic layer was shown analytically to have two ranges: the convective range and the dynamic range, as hypothesized by (Tong and Nguyen 2015). As part of a comprehensive analytical derivation of the MMO scaling properties of the surface-layer statistics from first principles, Tong and Ding (2020) also derived the mean velocity profile using the method of matched asymptotic expansions.

While the shear-stress and temperature-flux cospectra in the inertial range have been studied (e.g., Wyngaard et al. 1971), their scaling in the dynamic and convective range have not been predicted. In the present work, we use the MMO framework as well as the same physical arguments leading to MMO theory to predict the shear-stress cospectrum and temperature-flux cospectra in the MMO scaling region. The prediction is shown in Sect. 2. It is then compared to LES data in Sect. 3, which is followed by the conclusions.

2 Cospectra prediction

In this section, we use MMO theory (Tong and Nguyen 2015; Tong and Ding 2019) to predict the shear-stress and temperature-flux cospectra in the convective atmospheric surface layer for wavenumbers $kz < 1$, i.e., scales larger than z.

The governing parameters for the surface-layer statistics are u_*, Q, g/Θ, z and k, leading to two non-dimensional independent parameters, kL and z/L, since in MMO theory the Obukhov length L is not only a vertical length scale, but also a horizontal length scale. As shown in the MMO scaling regions in Fig. 1, there are two scaling ranges in the convective–

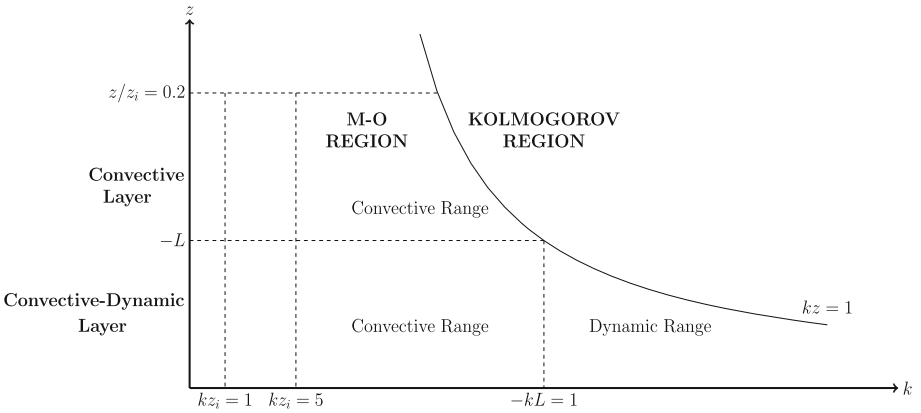

Fig. 1 Schematic of the scaling regions, layers, and ranges in the convective atmospheric surface layer. From Tong and Nguyen (2015) with permission

dynamic layer ($-z/L \ll 1$). The physical argument for the scaling is that the large-scale motions (low wavenumbers) in the convective–dynamic layer are coupled with motions in the convective layer ($-z/L \gg 1$). This coupling results from the nonlocal pressure transport and pressure–strain-rate correlation (Tong and Nguyen 2015).

Based on this physical argument, for the surface-layer eddies with a wavenumber $k \ll -1/L$ (i.e., the convective range), the velocity fluctuations at heights $z \ll 1/k$ are generated by the downward pressure transport and the pressure–strain-rate correlation (Ding et al. 2018). Specifically, the large eddies carry the velocity fluctuations downward from the height $z_p \sim 1/k$. At z_p, eddies of scale $1/k = z_p$ have the dominant contribution to the shear stress and the temperature fluxes (i.e., $z_p = 1/k$ is the production height for eddies of scale $1/k$). The shear stress and the horizontal temperature flux scale as (Wyngaard et al. 1971)

$$\overline{uw} \sim u_* \phi_m(\frac{z_p}{L}) u_f, \ \overline{u\theta} \sim u_* \phi_m(\frac{z_p}{L}) \frac{Q}{u_*} \phi_h(\frac{z_p}{L}), \tag{1}$$

where u_f is the local-free-convection velocity scale. According to Eq. 1, the magnitude of the mean-shear generated u fluctuations that are correlated with the w fluctuations at height $z_p = 1/k$ is

$$u \sim u_* \phi_m(\frac{z_p}{L}) \sim u_* (-\frac{z_p}{L})^{-\frac{1}{3}}, \tag{2}$$

where $(-z_p/L)^{-\frac{1}{3}}$ is the local free convection scaling of ϕ_m (Wyngaard et al. 1971). The magnitudes of the w and θ fluctuations are

$$w \sim u_f\big|_{z=z_p} \sim u_* (-\frac{z_p}{L})^{\frac{1}{3}} \tag{3}$$

and

$$\theta \sim \frac{Q}{u_*} \phi_h(\frac{z_p}{L}) \sim \frac{Q}{u_*} (-\frac{z_p}{L})^{-\frac{1}{3}}, \tag{4}$$

respectively. Because the fluctuations at the height $z_p = 1/k$ are carried downward by the large eddies to heights $z \ll 1/k$, the magnitude of the u fluctuation of the large eddies (i.e., the convective range, $-kL \ll 1$) at heights $z \ll 1/k$ is

$$u_c \sim u_* \phi_m(\frac{z_p}{L}) = u_* \phi_m(1/kL) \sim u_* (-kL)^{\frac{1}{3}}. \tag{5}$$

The magnitude of the w fluctuations in the convective range at heights $z \ll 1/k$ is,

$$w_c \sim u_f kz \sim u_*(-\frac{z_p}{L})^{\frac{1}{3}} kz \sim u_*(-kL)^{-\frac{1}{3}} kz. \tag{6}$$

Here wall blocking (continuity) reduces the w fluctuation by a factor of $kz \ll 1$ (Tong and Nguyen 2015). Therefore, in the convective range, the shear-stress (uw) cospectrum is

$$kC_{uw} \sim u_c w_c \sim u_*^2 kz, \tag{7}$$

$$\frac{C_{uw}}{u_*^2 z} = const. \tag{8}$$

The magnitude of the θ fluctuations of the large eddies (i.e.,those in the convective range, $-kL \ll 1$) is

$$\theta_c \sim \frac{Q}{u_f(z_p)} = \frac{Q}{u_f(1/k)} = \frac{Q}{u_*}(-kL)^{\frac{1}{3}}. \tag{9}$$

Thus, the $w\theta$ cospectrum in the convective range is

$$kC_{w\theta} \sim w_c \theta_c = Qkz, \tag{10}$$

$$\frac{C_{w\theta}}{Qz} = const. \tag{11}$$

The $u\theta$ cospectrum in the convective range is

$$kC_{u\theta} \sim u_c \theta_c \sim Q(-kL)^{\frac{2}{3}}, \tag{12}$$

$$-\frac{C_{u\theta}}{QL} \sim (-kL)^{-\frac{1}{3}}. \tag{13}$$

In the dynamic range ($-kL \gg 1$, $kz \ll 1$), the eddies are dominated by the mean shear effects. The horizontal velocity fluctuation u_d generated by the local mean shear is

$$u_d \sim \frac{\partial U}{\partial z} z \sim u_*. \tag{14}$$

The vertical velocity fluctuations w_d scale as $u_* kz$. Therefore the uw cospectrum in the dynamic range is

$$kC_{uw} \sim u_*^2 kz, \tag{15}$$

$$\frac{C_{uw}}{u_*^2 z} = const. \tag{16}$$

The temperature fluctuations in the dynamic range θ_d scale as Q/u_*. Thus, the $w\theta$ cospectrum in the dynamic range is

$$kC_{w\theta} \sim w_d \theta_d \sim Qkz, \tag{17}$$

$$\frac{C_{w\theta}}{Qz} = const. \tag{18}$$

Similarly, the $u\theta$ cospectrum in the dynamic range is

$$kC_{u\theta} \sim u_d \theta_d \sim Q, \tag{19}$$

$$\frac{C_{u\theta}}{Qz} \sim (kz)^{-1}. \tag{20}$$

The predicted cospectra are summarized in Fig. 2.

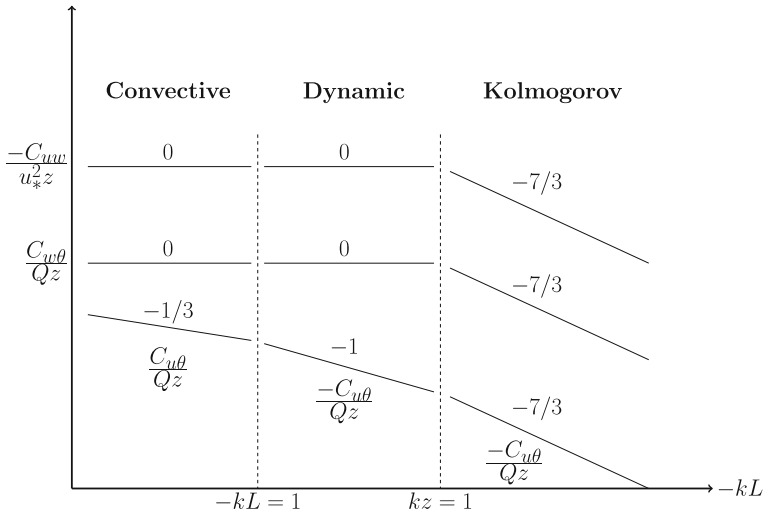

Fig. 2 Schematic of the predicted scaling (exponents) of the shear-stress cospectrum and temperature-flux cospectra, nondimensionalized by $u_*^2 z$ and Qz, respectively

3 Comparisons with LES

In this section we compare the cospectral predictions with LES of the atmospheric boundary layer (ABL). The LES formulation we used is described in detail in Moeng (1984) and has been well documented in the literature (Moeng and Wyngaard 1988; Sullivan et al. 1994, 1996), including later refinements by Otte and Wyngaard (2001). The simulated ABL is topped by a capping inversion layer. The initial value of the temperature is 308 K at the top of the capping inversion and 300 K within the ABL. The boundary layer then develops with a constant surface temperature flux and geostrophic wind. We simulate several cases of the ABL with different sets of the geostrophic wind speeds and surface heat flux with the parameters summarized in Table 1. The (nearly) neutrally stratified ABL is driven by a constant large-scale pressure-gradient corresponding to geostrophic wind components $(U_g, V_g) = (10, 0)$ m s^{-1} with zero surface heat flux. Three convective ABL simulations are driven by a combination of geostrophic wind speeds ($U_g = 8,\ 10,\ 15$ m s^{-1}) and surface heating ($Q = 0.08,\ 0.12,\ 0.20$ K m s^{-1}), respectively. The strongly convective boundary layer (CBL) is driven by a constant heat flux ($Q = 0.24$ K m s^{-1}) and weak geostrophic winds. In order to understand any effects of subgrid-scale (SGS) parameterization on the cospectra forms, we employed two SGS models: the Smagorinsky model (Smagorinsky 1963; Lilly 1967; Moeng 1984) and the Kosović model (Kosović 1997). The simulations are implemented on a mesh of 1024^3 and 2048^3 grid points, with a domain size of 5120^2 m^2 in the horizontal direction and 2048 m in the vertical direction. We also use the LES results to evaluate the non-dimensional coefficients of the shear-stress and vertical temperature-flux cospectra for these convective cases, which are summarized in Table 2. We run the simulations for 25 τ, where $\tau = z_i/w_*$ defines the large-eddy turnover time and $w_* = (\beta Q z_i)^{1/3}$ is the mixed-layer (Deardorff) velocity scale. The statistics are calculated by averaging from 10 τ to 25 τ.

We first compare the cospectra for the neutral cases obtained from LES to our predictions. The uw cospectra in the neutral surface layer obtained using the Smagorinsky and Kosović

Table 1 Large-eddy simulation parameters. (Simulations with * are implemented with 2048^3 grid points;) w_* is the mixed-layer (Deardorff) velocity scale

SGS model	U_g (m s^{-1})	Q (K m s^{-1})	u_* (m s^{-1})	$-L$ (m)	z_i (m)	w_* (m s^{-1})	$-z_i/L$ (1)
Smagorinsky	10	0	0.45	∞	981	0	0
Kosović	10	0	0.52	∞	984	0	0
Kosović	15	0.08	0.70	331	1015	1.38	3.07
Smagorinsky	15	0.08	0.65	262	1017	1.38	3.88
Kosović	10	0.12	0.55	104	1031	1.59	9.91
Kosović*	10	0.12	0.54	104	957	1.55	9.17
Smagorinsky	10	0.12	0.51	84	1032	1.59	12.29
Smagorinsky*	10	0.12	0.49	79	963	1.55	12.25
Smagorinsky	10	0.20	0.53	57	1040	1.88	18.2
Smagorinsky	8	0.20	0.46	38	1072	1.90	27.9
Smagorinsky	1	0.24	0.24	4	1076	2.02	259.9
Kosović	1	0.24	0.23	4	1074	2.02	267.2

Table 2 Nondimensional coefficients for the shear-stress and vertical temperature-flux cospectrum in the convective range (C. R.) and dynamic range (D. R.) from LES results

SGS model	Q (K m s^{-1})	U_g (m s^{-1})	C_{uw} C. R.	C_{uw} D. R.	$C_{w\theta}$ C. R.	$C_{w\theta}$ D. R.
Smagorinsky	10	0	–	0.22	–	–
Kosović	10	0	–	0.15	–	–
Kosović	15	0.08	0.28	0.33	0.32	0.32
Smagorinsky	15	0.08	0.30	0.30	0.34	0.34
Kosović	10	0.12	0.28	0.38	0.40	0.40
Kosović*	10	0.12	0.36	0.36	0.50	0.42
Smagorinsky	10	0.12	0.25	0.36	0.43	0.43
Smagorinsky*	10	0.12	0.36	0.36	0.60	0.44
Smagorinsky	10	0.20	0.25	0.36	0.46	0.46
Smagorinsky	8	0.20	0.25	0.36	0.46	0.46
Smagorinsky	1	0.24	0.15	–	0.47	–
Kosović	1	0.24	0.16	–	0.52	–

models at $z = 16,\ 20,$ and 30 m are shown in Fig.3. The cospectrum in the dynamic range ($1/z_i \ll k \ll 1/z$), predicted to have k^0 scaling, is more evident for the Smagorinsky model at $z = 30$ m, where the numerical resolution is better than at smaller heights. The cospectrum is approximately flat from wavenumber $kz = 1$ down to $kz = 3 \times 10^{-2}$. The nondimensional coefficients for C_{uw} in the dynamic range in the neutral surface layer obtained using the Smagorinsky and Kosović models are 0.22 and 0.15, respectively. Hunt and Carlotti (2001) and Högström et al. (2002) have also predicted the k^0 dependence of the shear-stress spectrum in a neutral ABL. Since there is no surface temperature flux in the neutral surface layer, we compare the $u\theta$ and $w\theta$ cospectra in the dynamic range later for the convective surface layer.

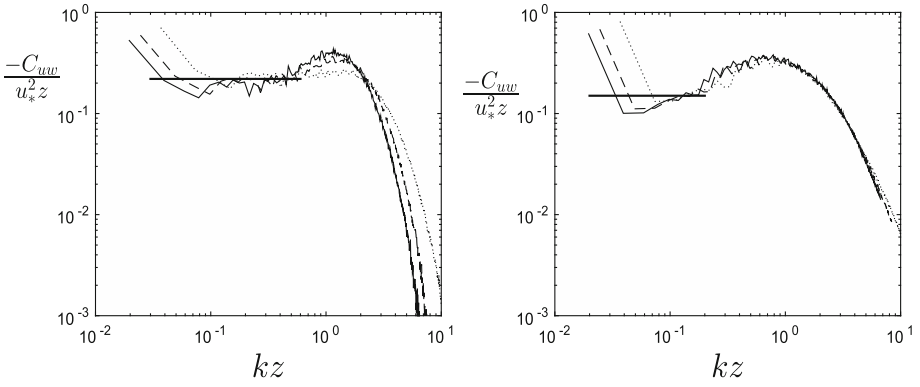

Fig. 3 Shear-stress cospectrum for the neutral ABL ($Q = 0$) from LES using the Smagorinsky SGS model (left) and the Kosović SGS (right) model, normalized by $u_*^2 z$. The lines represent heights of 16 (solid), 20 (dashed), and 30 m (dotted) hereafter

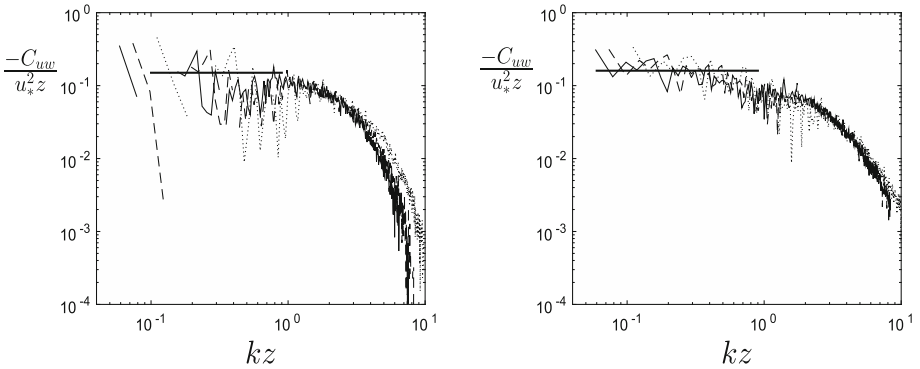

Fig. 4 Shear-stress cospectrum for the nearly-free convective ABL ($Q = 0.24$ K m s^{-1}) from LES using the Smagorinsky model (left) and the Kosović (right) model, non-dimensionalized by $u_*^2 z$

For the convective range ($-kL \ll 1$), the uw cospectrum is also predicted to have k^0 scaling, which is consistent with the LES results in the nearly-free convective surface layer shown in Fig. 4. The non-dimensional coefficients for C_{uw} in the convective range are shown to be 0.15 and 0.16 for the Smagorinsky model and Kosović model, respectively. There is a transition region (near $kz = 1$) between the convective range and inertial subrange. The $w\theta$ cospectrum is predicted to have k^0 scaling, and is also consistent with the LES results shown in Fig. 5. The nondimensional coefficients for $C_{w\theta}$ in the convective range are shown to be 0.47 and 0.52 for the Smagorinsky model and Kosović model, respectively. The $u\theta$ cospectrum is found to change sign in the convective range, and will be addressed later.

Our predictions of the shear-stress and temperature-flux cospectra in the convective-dynamic layer are tested by a series of CBL simulations (Figs. 6 to 9), with different surface temperature flux $Q = 0.08,\ 0.12,\ 0.20$ K m s^{-1}. The moderately convective surface layer ($Q = 0.12$ K m s^{-1}) is also investigated with a higher resolution (2048^3 grid points). The cospectra obtained from LES are shown in Figs. 6 to 9. The uw and $w\theta$ cospectra both have the predicted k^0 scaling in the convective and dynamic range. The weakly convective surface layer ($Q = 0.08$ K m s^{-1}) has a less extended convective range ($kz < 10^{-1}$, i.e., $-kL < 1$),

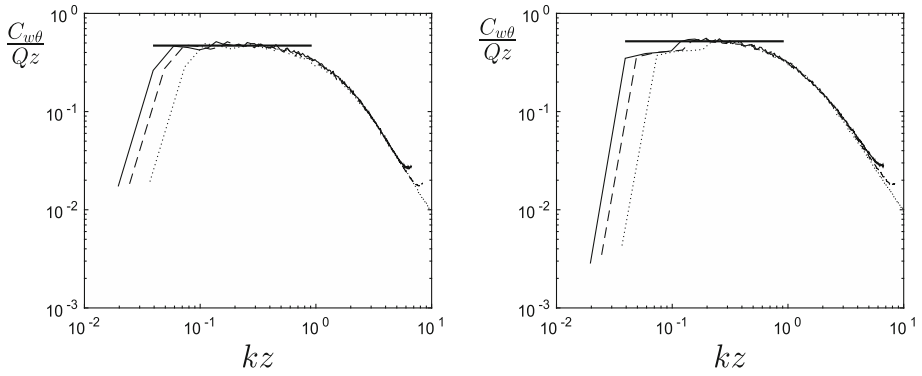

Fig. 5 $u\theta$ cospectrum for the nearly-free convective ($Q = 0.24$ K m s^{-1}) ABL from LES using the Smagorinsky model (left) and the Kosović (right) model, nondimensionalized by Qz

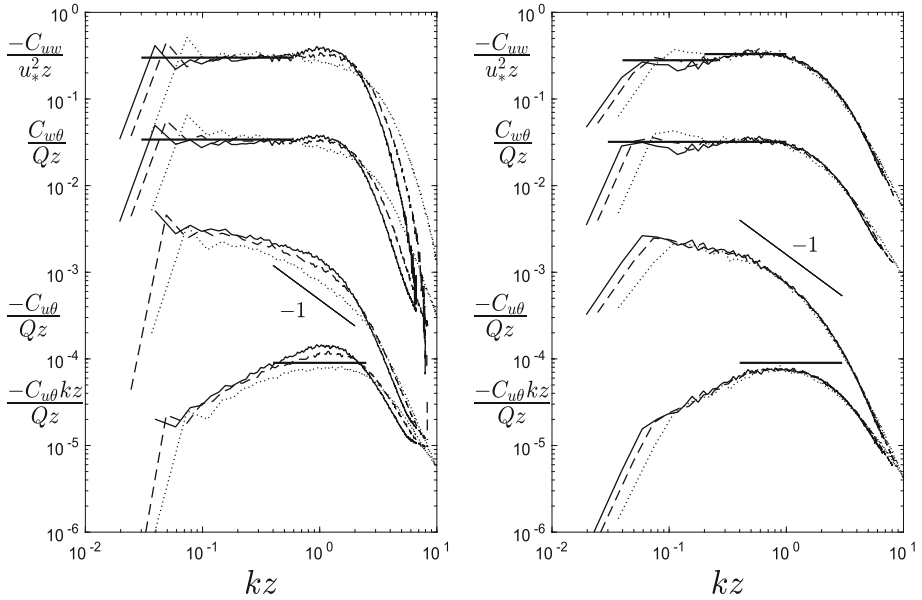

Fig. 6 Shear-stress cospectrum and temperature-flux cospectra in the weakly-convective ABL ($Q = 0.08$ K m s^{-1}) from LES using the Smagorinsky (left) and the Kosović (right) model, normalized by $u_*^2 z$ and Qz, respectively. For clarity, $C_{u\theta}$ and $C_{w\theta}$ have been multiplied by 1×10^{-3} and 1×10^{-1}, respectively. The values of kz where $-kL = 1$ for 16 m, 20 m, and 30 m are 0.06, 0.08, and 0.11, respectively, for the Smagorinsky model. The values of kz where $-kL = 1$ for 16 m, 20 m, and 30 m are 0.05, 0.06, and 0.09, respectively, for the Kosović model

compared to the moderately case ($kz < 2 \times 10^{-1}$) and the $Q = 0.20$ K m s^{-1} convective case ($kz < 3 \times 10^{-1}$).

The $u\theta$ cospectrum in the dynamic range appears to have a scaling range just to the left of $kz = 1$ in Figs. 6 to 9), with the scaling range more evident in Fig. 6. We have also plotted the cospectrum pre-multiplied by kz, which indicates that the slope of the cospectrum is less steep than k^{-1}. The $u\theta$ cospectrum in the convective surface layer with $Q = 0.20$ K m s^{-1} and the nearly-free convective surface layer obtained using LES is shown in Figs. 10

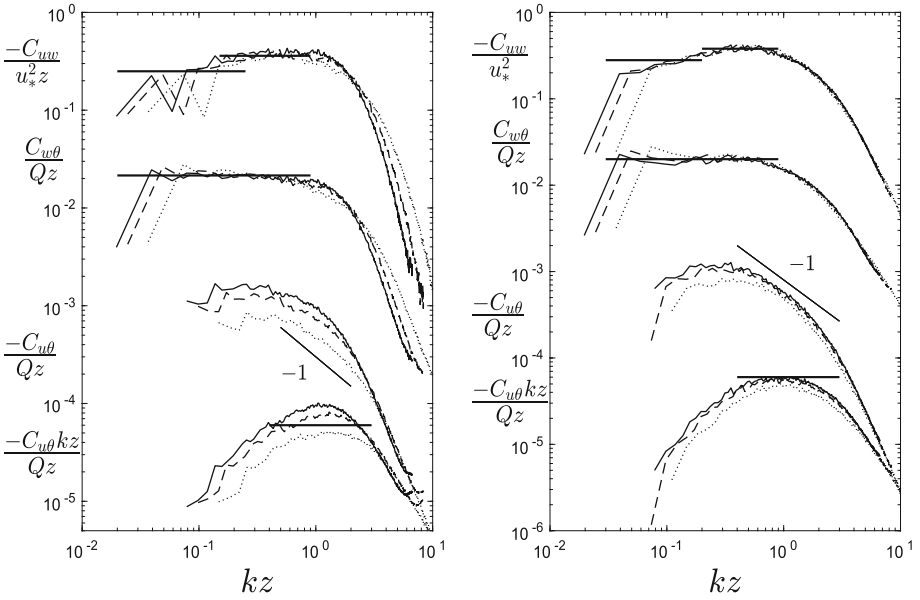

Fig. 7 Shear-stress cospectrum and temperature-flux cospectra in the moderately-convective ABL ($Q = 0.12$ K m s^{-1}) from LES using the Smagorinsky model (left) and the Kosović (right) model, nondimensionalized by $u_*^2 z$ and Qz, respectively. For clarity, $C_{u\theta}$ and $C_{w\theta}$ have been multiplied by 1×10^{-3} and 5×10^{-2}, respectively. The values of kz where $-kL = 1$ for 16 m, 20 m, and 30 m are 0.19, 0.24, and 0.36, respectively, for the Smagorinsky model. The values of kz where $-kL = 1$ for 16 m, 20 m, and 30 m are 0.15, 0.19, and 0.29, respectively, for the Kosović model

and 11, respectively. They are negative in the dynamic range but become positive in the convective range, with the crossover wavenumber $-kL \sim 2 \times 10^{-1}$. Although the scaling of $C_{u\theta}$ in the convective range is predicted to be $k^{-1/3}$, because of this sign change, a wider convective range is likely needed for the cospectrum to display a definitive scaling range. As a result, the cospectrum is steeper than $k^{-1/3}$ as it approaches the crossover. In the series of CBL simulations (Figs. 6 to 9), simulated, a significant range of wavenumbers is close to the crossover; therefore both the dynamic range and convective range are not sufficiently wide to determine the scaling exponents. A prediction using matched asymptotic expansions including the second order terms are likely needed to match the LES results.

The values of the spectral coefficients determined using the Smagorinsky and Kosović models are generally consistent. However, in LES there are fewer statistically independent large-scale fields than small-scale fields. The statistical uncertainties are higher for the large scales and for the convective-range cospectral coefficients. To obtain more accurate values field measurements are needed.

To understand the physics behind the positive $u\theta$ cospectrum in the convective range and the sign change, we compute the temperature–pressure-gradient cospectrum, which is a key term in the $u\theta$ cospectrum budget equation

$$\frac{DC_{u\theta}}{Dt} + C_{w\theta}\frac{\partial U}{\partial x_3} + C_{uw}\frac{\partial \Theta}{\partial x_3} + C_{tt} + C_{\theta \frac{\partial p}{\partial x}} = 0, \tag{21}$$

where the terms are the material derivative following the mean flow, the production by mean shear tilting and mean temperature gradient, the cospectral terms corresponding to

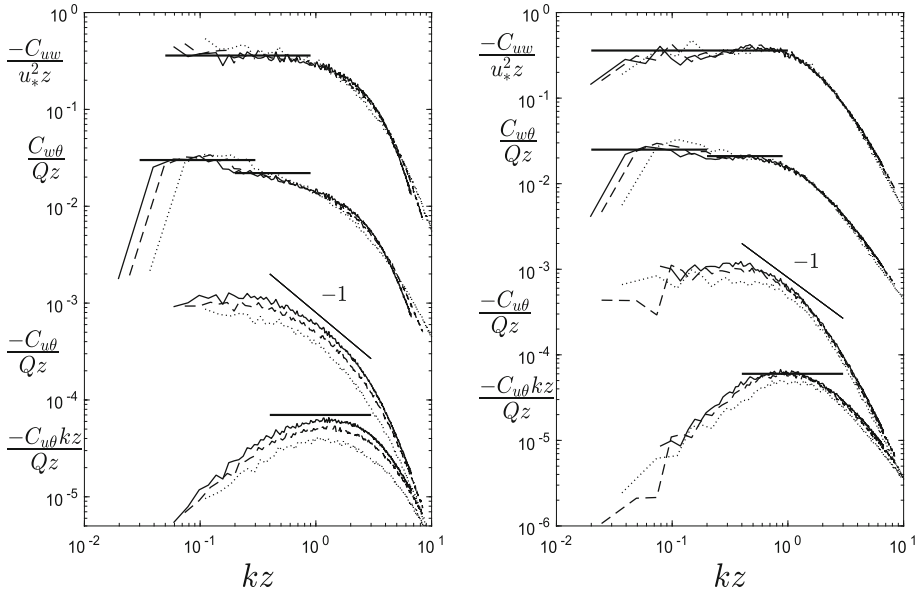

Fig. 8 Shear-stress cospectrum and temperature-flux cospectra in the moderately-convective ABL ($Q = 0.12$ K m s^{-1}) from LES using the Smagorinsky model (left) and the Kosović (right) model with 2048^3 resolution, nondimensionalized by $u_*^2 z$ and Qz, respectively. For clarity, $C_{u\theta}$ and $C_{w\theta}$ have been multiplied by 1×10^{-3} and 5×10^{-2}, respectively. The values of kz where $-kL =$ for 16 m, 20 m, and 30 m are 0.20, 0.25, and 0.38, respectively, for the Smagorinsky model. The values of kz where $-kL = 1$ for 16 m, 20 m, and 30 m are 0.15, 0.19, and 0.29, respectively, for the Kosović model

the turbulent transport term $\partial \overline{uw\theta}/\partial z$ and the temperature–pressure-gradient cospectrum. In both the dynamic and convective ranges, the temperature–pressure-gradient cospectrum is negative (Figs. 12 and 13). Therefore, it is a loss in the dynamics range, but is a dominant source in the convective range. This result indicates that the positive $u\theta$ cospectrum in the convective range is due to the pressure transport and the pressure–strain-rate correlation. The horizontal temperature flux produced at $z_p = 1/k$ by the mean shear and the mean temperature gradient is transported to $z \ll 1/k$. This physics is consistent with that leading to MMO theory. However, the direction of the flux at $z \ll 1/k$ is reversed compared to that at $z \sim 1/k$, apparently due to the eddy turnover, resulting in a positive temperature-flux cospectrum. This result further demonstrates the important role played by pressure in the dynamics of the convective surface layer.

4 Conclusions

In the present work, we predict the shear-stress cospectrum and the temperature-flux cospectra in the convective atmospheric surface layer using the MMO framework (Tong and Nguyen 2015; Tong and Ding 2019). In the Monin-Obukhov region, there are two scaling ranges in the convective–dynamic layer ($z \ll -L$): the convective range ($k \ll -1/L$) and the dynamic range ($-1/L \ll k \ll 1/z$), while there is only the convective range in the convective layer ($z \gg -L$). The turbulent fluctuations in the convective range in the convective–dynamic layer are coupled with those in the convective layer through large convective eddies. The

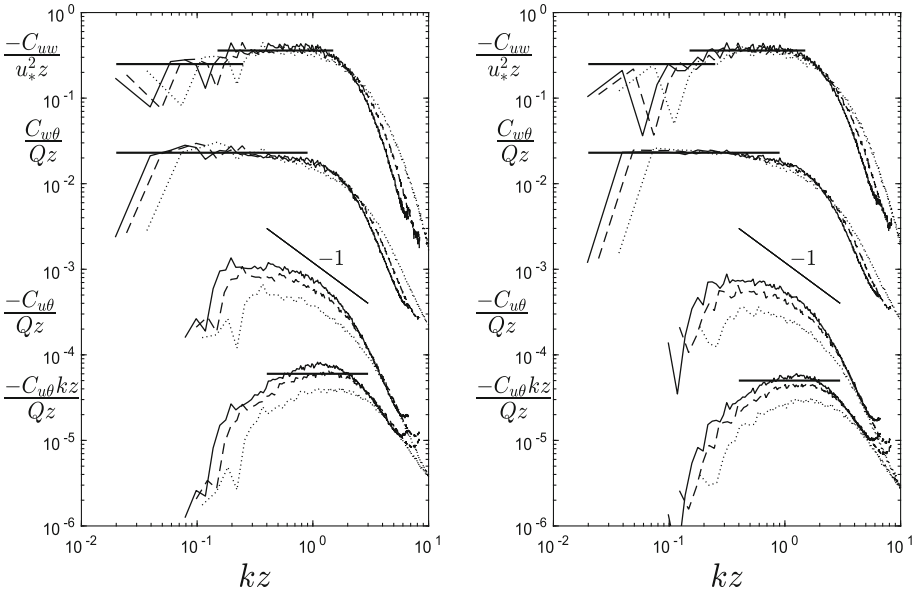

Fig. 9 Shear-stress cospectrum and temperature-flux cospectra in the CBL ($Q = 0.20$ K m s^{-1}) from LES using the Smagorinsky model with $U_g = 10$ m s^{-1} (left) and $U_g = 8$ m s^{-1} (right), nondimensionalized by $u_*^2 z$ and Qz, respectively. For clarity, $C_{u\theta}$ and $C_{w\theta}$ have been multiplied by 1×10^{-3} and 5×10^{-2}, respectively. The values of kz where $-kL = 1$ for 16 m, 20 m, and 30 m are 0.28, 0.35, and 0.53, respectively, for the Smagorinsky model. The values of kz where $-kL = 1$ for 16 m, 20 m, and 30 m are 0.42, 0.53, and 0.79, respectively, for the Kosović model

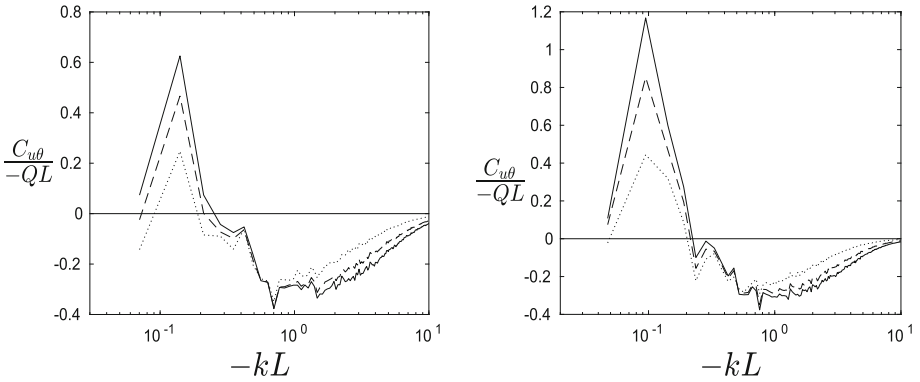

Fig. 10 $u\theta$ cospectrum for the convective ($Q = 0.20$ K m s^{-1}) ABL from LES using the Smagorinsky model with $U_g = 10$ m s^{-1} (left) and $U_g = 8$ m s^{-1} (right), non-dimensionalized by $-QL$

fluctuations are generated by the pressure transport and the pressure–strain-rate, which are carried downward by the large eddies from the convective layer. Thus, the cospectra forms in the convective range for the convective layer and the convective–dynamic layer are the same. In the dynamic range, the eddies are dominated by the shear effects, and the fluctuations are generated by the mean shear.

The shear-stress cospectrum (C_{uw}) and the $w\theta$ cospectrum ($C_{w\theta}$) are predicted to have k^0 scaling in both the convective range and the dynamic range. The $u\theta$ cospectrum ($C_{u\theta}$) is

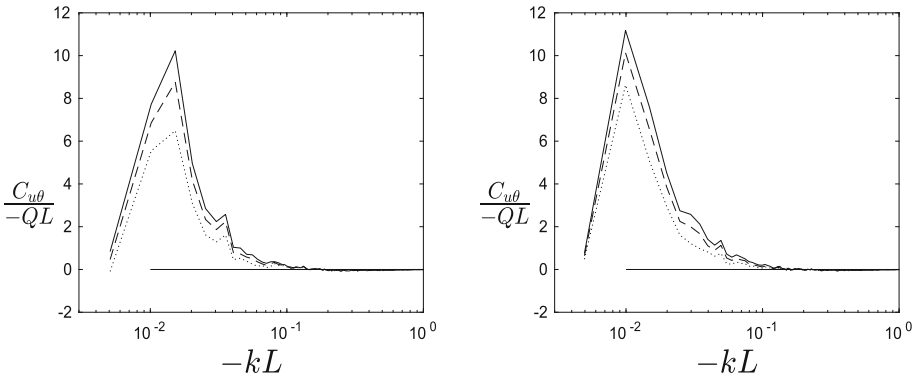

Fig. 11 Horizontal temperature-flux cospectrum for the nearly free-convective ($Q = 0.24$ K m s^{-1}) ABL from LES using the Smagorinsky model (left) and the Kosović (right) model, nondimensionalized by $-QL$

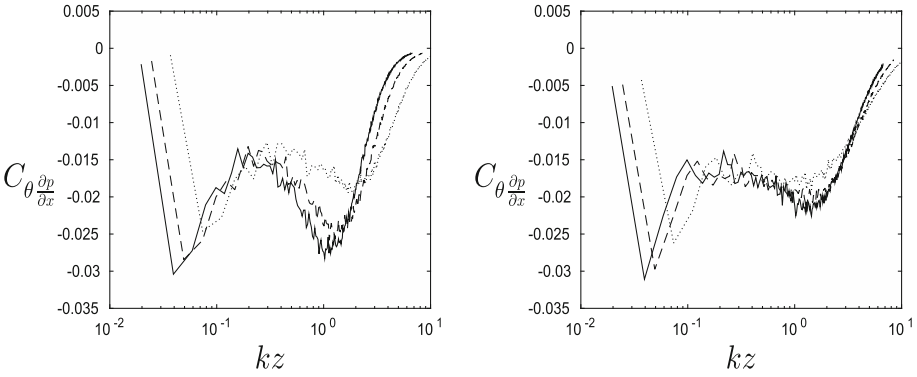

Fig. 12 Temperature–pressure-gradient cospectrum in the moderately convective ABL ($Q = 0.12$ K m s^{-1}) from LES using the Smagorinsky (left) model and the Kosović (right) model, respectively

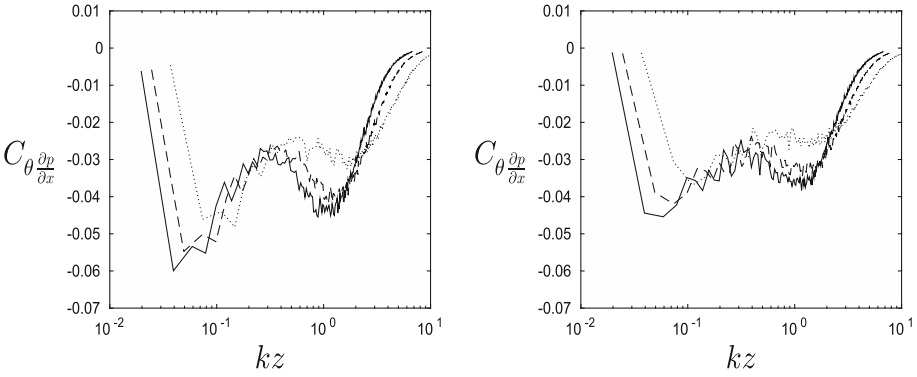

Fig. 13 Temperature–pressure-gradient cospectrum in the CBL ($Q = 0.20$ K m s^{-1}) from LES using the Smagorinsky model with $U_g = 10$ m s^{-1} (left) and $U_g = 8$ m s^{-1} (right), respectively

predicted to have $k^{-1/3}$ and k^{-1} scaling in the convective range and dynamic range, respectively. However, the sign of $C_{u\theta}$ changes from negative in the dynamic range to positive in the convective range, with the crossover being at $-kL \sim 2 \times 10^{-1}$. An analysis of the temperature–pressure-gradient cospectrum in the $C_{u\theta}$ budget equation shows that this sign change is due to the pressure effects associated with the convective eddies. The predicted cospectral scaling exponents are in general agreement with the large-eddy simulation results. Because of the sign change of $C_{u\theta}$, the cospectrum appears steeper than $-1/3$ when approaching the crossover. The cospectrum in the dynamic range is also affected by the sign change. Thus, wider convective and dynamic ranges of the cospectrum are likely needed to determine the scaling exponents. The cospectral coefficients are also obtained from LES using the Smagorinsky SGS model and the Kosović SGS model. While the cospectral coefficients are generally consistent between the models, the statistical uncertainties of the cospectral coefficients in the convective range are larger. Further comparisons with field measurements are needed to determine the coefficients with higher accuracy.

Acknowledgements We would like to acknowledge high-performance computing support from Cheyenne (doi:10.5065/D6RX99HX) provided by NCAR's Computational and Information Systems Laboratory, sponsored by the National Science Foundation. Clemson University is acknowledged for the generous allotment of compute time on Palmetto cluster. This work was supported by the National Science Foundation through grants no. AGS-1561190.

References

Betchov R, Yaglom AM (1971) Comments on the theory of similarity as applied to turbulence in an unstable stratified fluid. Izv Akad Nauk, Ser Fiz Atmos Okeana, English translation 7:829–832

Businger JA, Wyngaard JC, Izumi Y, Bradley EF (1971) Flux-profile relationships in the atmospheric surface layer. J Atmos Sci 28:181–189

Caughey SJ, Palmer SG (1979) Some aspects of turbulence structure through the depth of the convective boundary layer. QJR Met Soc 105:811–827

Ding M, Nguyen KX, Liu S, Otte M, Tong C (2018) Investigation of the pressure-strain-rate correlation and pressure fluctuations in convective and near neutral atmospheric surface layers. J Fluid Mech 854:88–120

Högström U (1988) Non-dimensional wind and temperature profiles in the atmospheric surface layer: A re-evaluation. Boundary-Layer Meteorol 42:55–78

Högström U (1990) Analysis of turbulence structure in the surface layer with a modified similarity formulation for near neutral conditions. J Atmos Sci 47:1949–1972

Högström U, Hunt JCR, Smedman AS (2002) Theory and measurements for turbulence spectra and variances in the atmospheric neutral surface layer. Boundary-Layer Meteorology 103:101–124

Hunt JCR, Carlotti P (2001) Statistical structure at the wall of the high reynolds number turbulent boundary layer. Flow, Turbulence and Combustion 66:453–475

Kader BA (1988) Three-layer structure of an unstably stratified atmospheric surface layer. Izv Akad Nauk, Ser Fiz Atmos Okeana, English translation 24:907–918

Kaimal JC (1978) Horizontal velocity spectra in an unstable surface layer. J Atmos Sci 35:18–24

Kaimal JC, Wyngaard JC, Izumi Y, Coté OR (1972) Spectral characteristic of surface-layer turbulence. QJR Met Soc 98:563–589

Kosović B (1997) Subgrid-scale modelling for the large-eddy simulation of high-Reynolds-number boundary layer. J Fluid Mech 336:151–182

Lilly DK (1967) The representation of small-scale turbulence in numerical simulation experiments. In: Goldstine HH (ed) Proc. IBM Scientific Computing Symp. on Environ. Sci, IBM, Yorktown heights, NY, pp 195–210

Lumley JL, Panofsky HA (1964) The Structure of Atmospheric Turbulence. Interscience Monographs and Texts in Physics and Astronomy, Vol. 12, Interscience, New York

Moeng CH (1984) A large-eddy simulation model for the study of planetary boundary-layer turbulence. J Atmos Sci 41:2052–62

Moeng CH, Wyngaard JC (1988) Spectral analysis of large-eddy simulations of the convective boundary layer. J Atmos Sci 45:3573–3587

Monin AS, Obukhov AM (1954) Basic laws of turbulent mixing in the ground layer of the atmosphere. Trans Inst Teoret Geofiz Akad Nauk SSSR 151:163–187
Nguyen KX (2015) On subgrid-scale physics in the convective atmospheric surface layer. Ph.D. dissertation, Clemson University, Department of Mechanical Engineering
Nguyen KX, Tong C (2015) Investigation of subgrid-scale physics in the convective atmospheric surface layer using the budgets of the conditional mean subgrid-scale stress and temperature flux. J Fluid Mech 772:295–329
Obukhov AM (1946) Turbulence in the atmosphere with inhomogeneous temperature. Trans Inst Teoret Geofiz Akad Nauk SSSR 1:95–115
Otte MJ, Wyngaard JC (2001) Stably stratified interfacial-layer turbulence from large-eddy simulation. J Atmos Sci 58:3424–3442
Smagorinsky J (1963) General circulation experiments with the primitive equations: I. The basic equations. Mon Weather Rev 91:99–164
Sullivan PP, McWilliams JC, Moeng CH (1994) A subgrid-scale model for large-eddy simulation of planetary boundary-layer flows. Boundary-Layer Meteorol 71:247–276
Sullivan PP, McWilliams JC, Moeng CH (1996) A grid nesting method for large-eddy simulation of planetary boundary-layer flows. Boundary-Layer Meteorol 80:167–202
Tong C, Ding M (2018) Monin-Obukhov similarity and local-free-convection scaling in the atmospheric boundary layer using matched asymptotic expansions. J Atmos Sci 75:3691–3701
Tong C, Ding M (2019) Multi-point Monin-Obukhov similarity in the convective atmospheric surface layer using matched asymptotic expansions. J Fluid Mech 864:640–669
Tong C, Ding M (2020) Velocity-defect laws, log law and logarithmic friction law in the convective atmospheric boundary layer. J Fluid Mech 883:A36
Tong C, Nguyen KX (2015) Multipoint Monin-Obukhov similarity and its application to turbulence spectra in the convective atmospheric surface layer. J Atmos Sci 72:4337–4348
Wyngaard JC, Coté OR (1971) The budgets of turbulent kinetic energy and temperature variance in the atmospheric surface layer. J Atmos Sci 28:190–201
Wyngaard JC, Coté OR, Izumi Y (1971) Local free convection, similarity, and the budgets of shear stress and heat flux. J Atmos Sci 28:1171–1182
Yaglom AM (1994) Fluctuation spectra and variances in convective turbulent boundary layers: A reevaluation of old models. Phys Fluids 6:962–972
Zilitinkevich SS (1971) On the turbulence and diffusion under free convection conditions. Izv Akad Nauk, Ser Fiz Atmos Okeana 7:1263–1269